

Supporting Information for

Generation of B-Doped Graphene Nano-Platelets Using Solution Process and Their Supercapacitor Applications

Jongwoo Han,^{†,□} Li Li Zhang,^{‡,□} Seungjun Lee,[†] Junghoon Oh,[†] Kyoung-Seok Lee,[§] Jeffrey R. Potts,[‡] Junyi Ji,[‡] Xin Zhao,[‡] Rodney S. Ruoff,[‡] and Sungjin Park^{†,*}

[†]Department of Chemistry, Inha University, 100 Inha-ro, Nam-gu, Incheon, 402-751 Korea,

[‡]Department of Mechanical Engineering and the Materials Science and Engineering

Program, The University of Texas at Austin, One University Station C2200, Austin, TX,

78712-0292 USA, Center for Analytical Chemistry, and [§]Korea Research Institute of

Standards and Science, Yuseong, Daejeon 305-340, Korea

* Corresponding author

Tel: +82-32-860-7677, Fax: +82-32-867-5604, e-mail: sungjinpark@inha.ac.kr

□ These authors equally contributed to this work

Effect of reaction time on the reduction behavior in B-rG-O systems

The B-rG-O powder (Fig. 1) was isolated by filtration with a glass-frit filter, then thoroughly washed with water then dried under vacuum at room temperature. Samples used in this work were allowed to react for 4 days under reflux. After 1 day of reaction time, the color of the reaction mixture had turned to black. Black agglomerated particles were visible in the reaction mixture after 2 days. However, the material obtained after 2 days of reaction showed a lower degree of reduction than the B-rG-O obtained after 4 days reaction time (Figure S1).

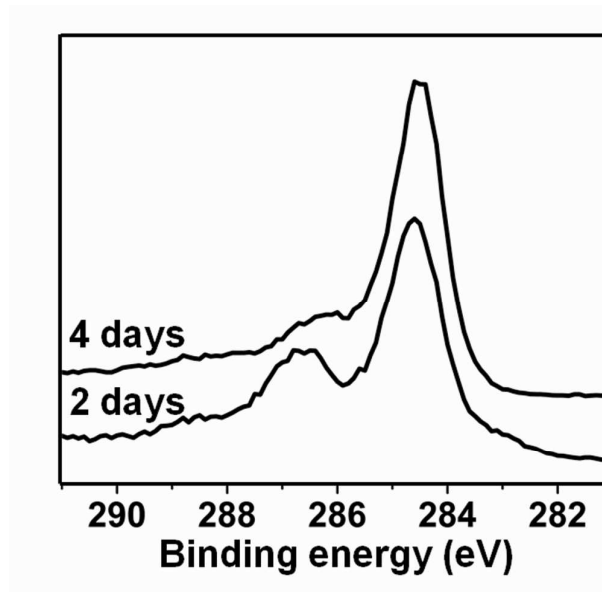


Figure S1. C1s XPS spectra of B-rG-O materials produced after 2 days and 4 days.

Preparation and analysis of B-G-O-80 and B-G-O-60.

An aqueous suspension (3 mg of GO/1 ml of water) of graphene oxide was produced as described above. A solution of borane-THF adduct (0.03 ml per 10 mg of GO) was added to the suspension with stirring. Then the flask was immersed in an oil bath set at 60 °C (for B-G-O-60) and separately 80 °C (for B-G-O-80) and the brown suspension was stirred for 4 days with a magnetic stirring bar, affording a dark brown suspension. To isolate B-G-O materials, the flask was cooled down at room temperature, then the suspension was filtered over an Anodisc membrane filter (47 mm in diameter, 0.02 μm pore size, Whatman) then washed with water (100 ml) at least 3 times. After drying under air for 24 h, the resulting

paper-like material was peeled off from the membrane and further dried under vacuum for 12 h.

We used a reflux condition of an aqueous system to produce B-rG-O in this work. However, when the reaction was done on an oil bath set at 80 °C, the product (henceforth, B-G-O-80) showed much different chemical identities than the B-rG-O reduced under reflux. Even after 4 days of reaction time, the product was only slightly darker than the initial brown suspension of graphene oxide nano-platelets and the resulting suspension of B-G-O-80 was still stable in water. The B-G-O-80 nano-platelets were isolated as a film by filtration using a membrane filter and it was found that it had a much lower degree of reduction than B-rG-O (Figure S2). The B-G-O-80 (C/O = 1.5), produced from the reaction at 80 °C, showed much lower degree of reduction than the B-rG-O. This suggests that the reaction temperature is a critical parameter in the reduction of graphene oxide with a borane-THF adduct. The C1s XPS spectrum of B-G-O-60, which was produced by treatment with borane-THF at 60 °C, also showed almost no degree of reduction. Due to the low degree of reduction, those samples were obtained as only colloidal suspensions. So, we could not prepare the samples as powder form, only obtained as paper-like materials. Consequently, we did not investigate the electrochemical performances of those samples.

In the B1s spectra, while the B-G-O-80, produced at 80 °C, showed a peak around 190 eV, the peak around 190 eV, which corresponds to BC moieties,⁴⁻⁷ was not observed in the spectrum of B-rG-O. The peaks at both 190 and 191 eV correspond to B-C bonds. From these data, we suggest that boron atoms are covalently attached to C atoms in graphene networks at 80 °C, while the boron atoms are incorporated into the sp² network when a reaction temperature of 100 °C is used.

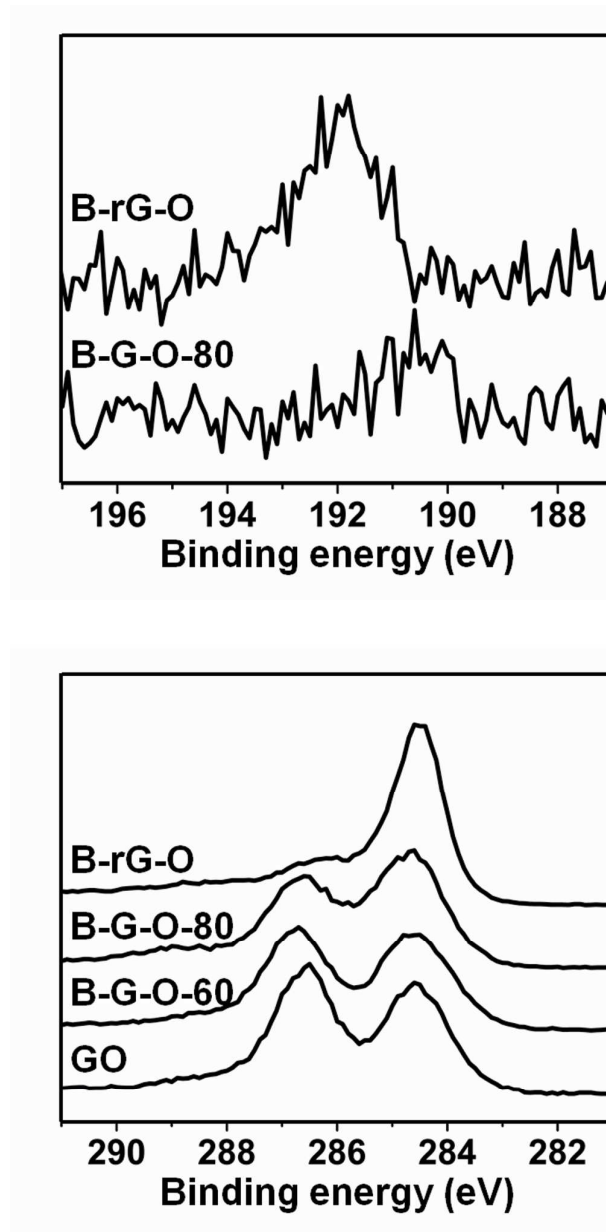


Figure S2. XPS spectra; (top), B1s region and (bottom) C1s region.

FT-IR measurement of B-rG-O and B-G-O-80

A C=C stretch of B-rG-O was significantly shifted to 1570 cm^{-1} from that of GO at 1610 cm^{-1} , while that of B-G-O-80 is almost the same as that of GO (Figure S3). This shift could be induced by a combination of increased conjugation of the sp^2 networks and the incorporation of B atoms into the sp^2 network in the B-rG-O sample.¹⁻³

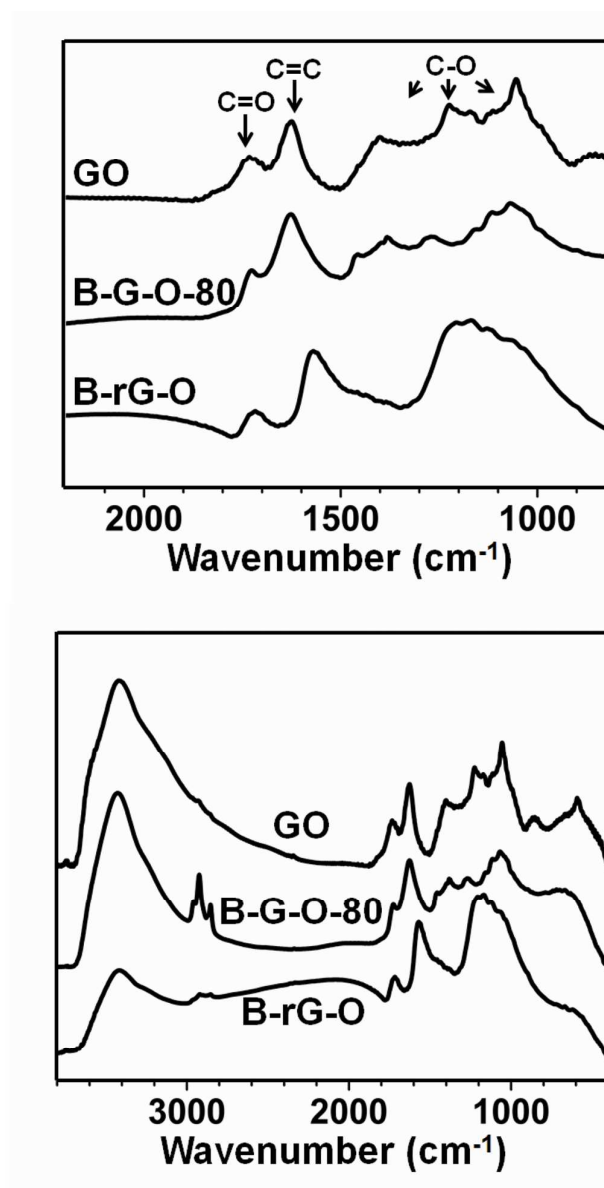


Figure S3. FT-IR spectra of GO, B-G-O-80, and B-rG-O, selected region (top) and full region (bottom).

Preparation and analysis of 4d-rG-O.

An aqueous suspension (3 mg of GO/1 ml of water) of graphene oxide was produced as described above. The flask was then immersed in an oil bath, and the brown suspension was stirred under reflux for 4 days. The resulting black solid product (4d-rG-O) was filtered and dried under vacuum at room temperature for 12 h, and a C/O ratio of 5.0 was obtained by elemental analysis, lower than that of B-rG-O (C/O ratio: 7.8). C1s XPS spectra also confirmed that the graphene oxide was reduced by 4 days of refluxing (Figure S4). The FT-IR spectrum of 4d-rG-O showed a decrease of peaks associated with oxygen functional groups relative to that of GO (Figure S5). However, the spectrum differs from that of B-rG-O showing that the borane species also plays an important role in the reduction of graphene oxide to produce B-rG-O.

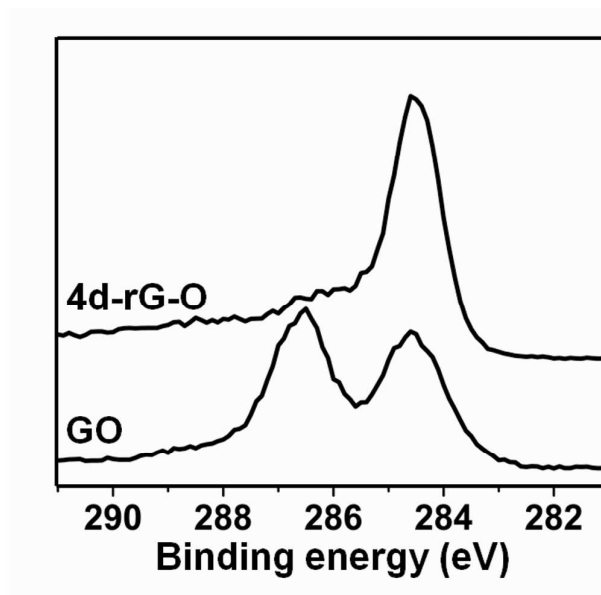


Figure S4. C1s XPS spectra of GO and 4d-rG-O.

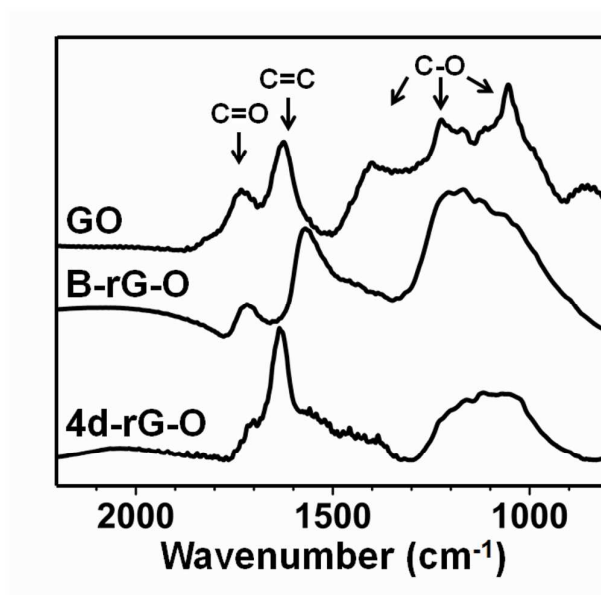


Figure S5. FT-IR spectra of GO, B-rG-O and 4d-rG-O at selected region.

ICP/MS experimental for measurements of boron content

The quantification of B content was carried out by ICP-MS, which is one of the most powerful tools for elemental quantification in a sub-ppm. ICP-MS measurements showed that the B-rG-O contained a small amount (0.11 wt%) of B.

About 12 mg of B-rG-O powder was weighed into the TFM vessel (ETHOS PLUS, Milestone Inc., USA) using a microbalance (AX26, Mettler-Toledo Inc., US) and 4 ml of 65 % nitric acid and 4 ml of 95 % sulfuric acid were added to each vessel. The vessels sealed by the outer closed vessel systems were placed in the microwave digestion system (ETHOS PLUS, Milestone Inc., USA). The reaction was controlled by the temperature with heating to 200 °C over 15 min and holding at 200 °C for 25 min. After a period of standing for cooling, 4 ml of 65 % nitric acid and 2 ml of 95 % sulfuric acid were added and microwave digestion using the same temperature program was carried out. The reaction cycle with addition of 4 ml of nitric acid and 2 ml of sulfuric acid followed by temperature controlled microwave digestion were repeated more than three times to check whether the samples had been digested completely. The excess nitric acid was evaporated between the cycles. Finally, microwave digestion with *aqua regia* was carried out to assure complete digestion. The clear solutions were transferred into LDPE bottles and diluted with water to appropriate concentration prior to ICP/MS measurements.

ICP/MS measurements were carried out using a Thermo Element2 magnetic sector type ICP-MS system (Thermo Fisher Scientific, German) with an O-ring free platinum injector, quartz torch, and cyclonic spray chamber and nebulizer made of perfluoroalkoxy (PFA) Teflon[®] (Elemental Scientific, USA). Both ¹⁰B and ¹¹B isotopes were measured at the medium resolution setting ($R > 4000$) and the isotopic abundance ratio of the two isotopes of boron showed good agreement with IUPAC reference values⁸ indicating no significant contributions from interference in the measurements. Standard solutions for external standard calibration were prepared from 1 g/kg B calibration solution of KRISS certified reference

material. The calibration curve generated by the ^{10}B response to the boron concentration was linear and had an R squared value of over 0.997.

Powder conductivity measurement.

The electrical resistance of as-prepared B-rG-O powders was determined using a glass tube with volume scale and two stainless steel rods, measured by a multi-meter. The electrical conductivity was determined by fitting the powder conductivity experimental data to the equation: $\sigma_c = \sigma_h [(\phi - \phi_c)/(1 - \phi_c)]^k$, with the assumption that the conductivity of the low-conductivity phase (air) is zero. σ_c is the conductivity of the composite medium, σ_h and ϕ are the conductivity of the conductive phase (the B-rG-O powder) and its volume fraction, respectively, ϕ_c is the percolation threshold, and k is a critical exponent related to the percolation threshold and to the shape of the particles. The percolation threshold, ϕ_c , is determined as a ratio of the apparent powder density before compression, d_p , and the apparent density of the particles, d_g . The bulk density of graphite (2.2 g/cm^3) has been used as a value for d_g . σ_c and ϕ were calculated from the parent volume of the B-doped CMG powders. Figure S6 shows σ_c values as a function of ϕ during the compression. The fitting curve gave the values of σ_h and k to be $\sim 50.4 \text{ S/m}$ and ~ 1.43 , respectively.

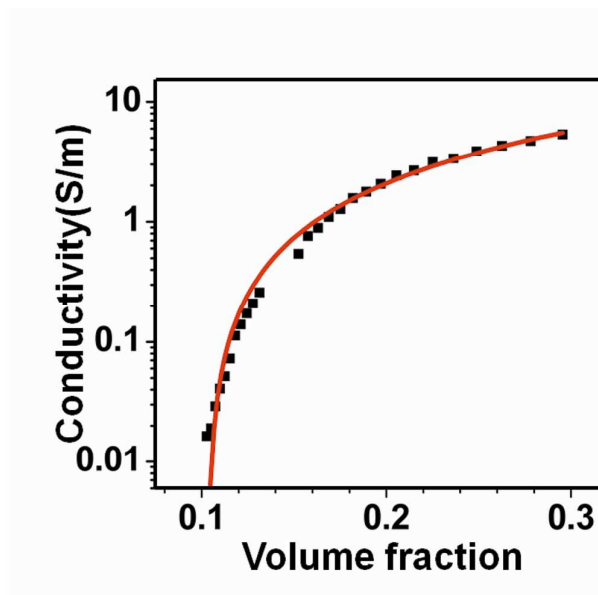


Figure S6. Powder conductivity measurement of B-rG-O sample.

Instruments

Elemental analysis was measured with a FLASH EA1112 instrument (Thermo Electron, Italia) under Helium atmosphere to determine C, N, O and H content. XPS were studied on Angle-Resolved X-ray Photoelectron Spectrometer (Theta probe, Thermo electron cooperation, UK) was conducted with a MXR1 Gun-400 um 15 kV spectrometer. The binding energy was referenced to the natural C1s peak at 284.6 eV. FT-IR spectra were collected on a KBr pellet of B-rG-O powder samples on a FT-IR Vacuum Spectrometer (Bruker VERTEX 80V, Bruker, Germany). Each spectrum, which was recorded as the average of 64 scans with a resolution of 4 cm^{-1} , was collected from 4000 cm^{-1} to 400 cm^{-1} . SEM images were obtained with a field emission gun scanning electron microscope (S-4300, Hitach, Japan) using an accelerating voltage of 15 kV. Thermogravimetric analysis (STA 409 PC, NETZSCH, Germany) was measured with $3\text{ }^{\circ}\text{C}/\text{min}$ heating rate between 30 and $800\text{ }^{\circ}\text{C}$ under argon atmosphere. BET surface area measurements (BELSORP-mini II, BEL Japan,

Inc., Japan) were performed with absorption of nitrogen. Micro Raman measurements of powder samples were carried out using a WiTec Alpha300 system with a 532 nm wavelength incident laser light.

Raman measurement. Raman spectra of both GO and B-rG-O powders contain two broad peaks around 1355 cm^{-1} , a D band from defects, and around 1595 cm^{-1} , a G band from sp^2 graphitic network. A comparable intensity of D band relative to that of the G band is typically observed from CMG materials because many defects are generated during harsh oxidation and sonication process.

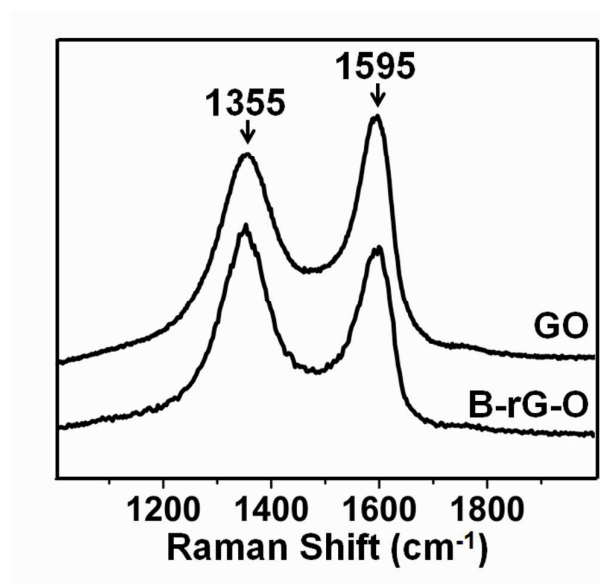


Figure S7. Raman spectra of GO and B-rG-O.

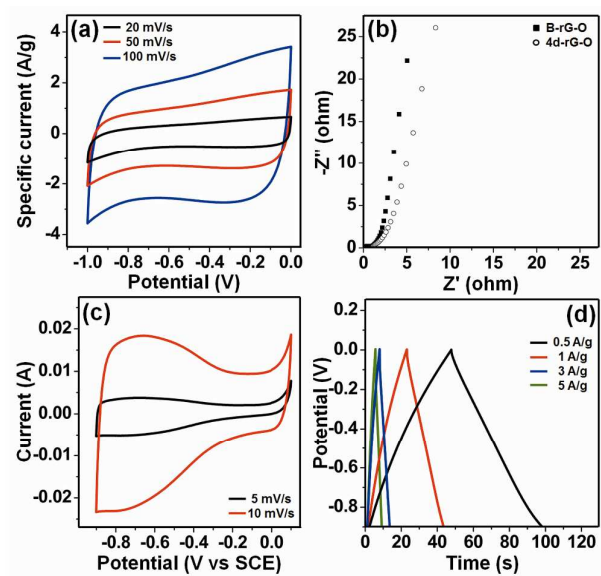


Figure S8. The electrochemical performance of 4d-rG-O electrode in 6M KOH solution using a two-electrode configuration, showing (a) CV curves at various scan rates, (b) Nyquist plots showing the imaginary part *versus* the real part of impedance. (c) CV curves at various scan rates using a three-electrode configuration, and (d) galvanostatic charge/discharge curves under different current densities.

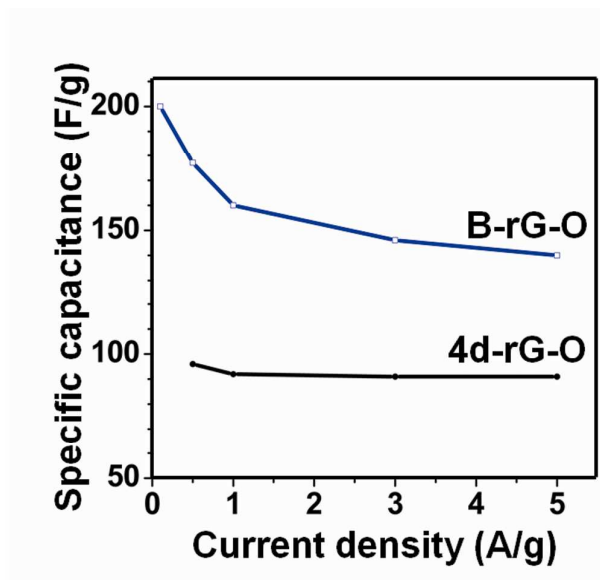


Figure S9. Gravimetric capacitance comparison between B-rG-O and 4d-rG-O electrodes at various scan rates using a two-electrode configuration.

Ragone plot.

The energy density was estimated by using the formula

$$E = \frac{C_{single} V^2}{8}$$

The effective series resistance (ESR) was estimated using the voltage drop at the beginning of the discharge, V_{drop} , at a certain constant current I , with the formula

$$R_{ESR} = \frac{V_{drop}}{2I}$$

The power density, calculated from the discharge data at this certain constant current I and normalized with the weight of the cell (two electrodes) is given by

$$P = \frac{(V_{max} - V_{drop})^2}{4R_{ESR}m}$$

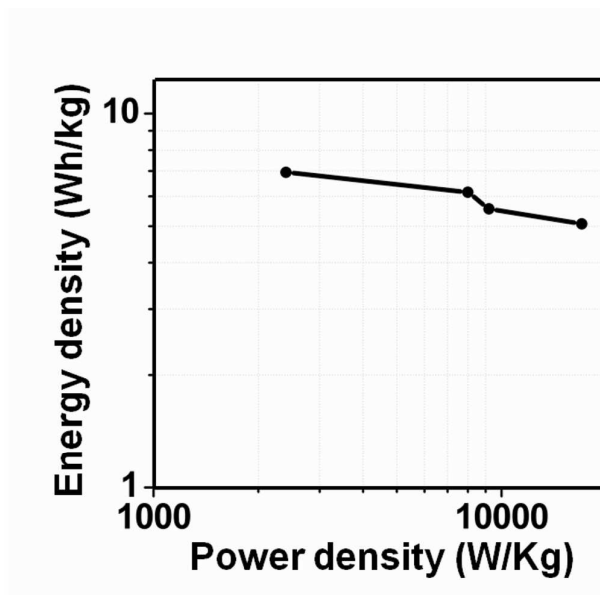


Figure S10. Ragone plot showing the energy density and power density for B-rG-O electrode in 6M KOH.

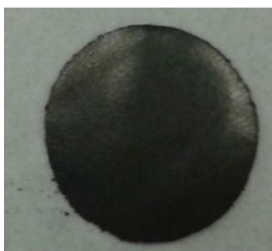


Figure S11. An image for the electrode in 2-electrode test



Figure S12. An image for the electrode in 3-electrode test

References

1. Moon, I.; Lee, J.; Ruoff, R. S.; Lee, H., Reduced graphene oxide by chemical graphitization. *Nat. Commun.* **2010**, 1, 73.
2. Park, S.; An, J.; Piner, R. D.; Jung, I.; Yang, D.; Velamakanni, A.; Nguyen, S. T.; Ruoff, R. S., Aqueous suspension and characterization of chemically modified graphene sheets. *Chem. Mater.* **2008**, 20, 6592-6594.
3. Nakamoto, K., *Infrared and raman spectra of inorganic and coordination compounds*. 4th ed.; John Wiley & Sons New York, Chichester, Brisbane, Toronto, Singapore, 1986.
4. Wang, J.; Chen, Y.; Zhang, Y.; Ionescu, M. I.; Li, R.; Sun, X.; Ye, S.; Knights, S., 3D boron doped carbon nanorods/carbon-microfiber hybrid composites: synthesis and applications in a highly stable proton exchange membrane fuel cell. *J. Mater. Chem.* **2011**, 21, 18195-18198.
5. Jacobsohn, L. G.; Schulze, R. K.; da Costa, M. E. H. M.; Nastasi, M., X-ray photoelectron spectroscopy investigation of boron carbide films deposited by sputtering. *Surf. Sci.* **2004**, 572, 418-424.
6. Panchakarla, L. S.; Subrahmanyam, K. S.; Saha, S. K.; Govindaraj, A.; Krishnamurthy, H. R.; Waghmare, U. V.; Rao, C. N. R., Synthesis, structure, and properties of boron- and nitrogen-doped graphene. *Adv. Mater.* **2009**, 21, 4726-4730.
7. Wu, Z.-S.; Ren, W.; Xu, L.; Li, F.; Cheng, H.-M., Doped graphene sheets as anode materials with superhigh rate and large capacity for lithium ion batteries. *ACS Nano* **2011**, 7, 5463-5471.
8. Cohen, E. R.; Cvitas, T.; Frey, J. G.; Holmstrom, B.; Kuchitsu, K.; Marquardt, R.; Mills, I.; Pavese, F.; Quack, M.; Stohner, J.; Strauss, H. L.; Takami, M.; Thor, A. J., *Quantities, units and symbols in physical chemistry*. 3rd ed.; RSE Publishing: Cambridge, 2007.

